Amorphous Carbon Bearing Sulfonic Acid Groups in Mesoporous Silica as a Selective Catalyst

Kiyotaka Nakajima,[†] Mai Okamura,[†] Junko N. Kondo,[‡] Kazunari Domen,[§] Takashi Tatsumi,[‡] Shigenobu Hayashi,[||] and Michikazu Hara*[,†,⊥]

Materials and Structures Laboratory, Tokyo Institute of Technology, 4259-R3-33, Nagatsuta-cho, Midori-ku, Yokohama 226-8503 Japan, Chemical Resources Laboratory, Tokyo Institute of Technology, 4259-R1-9, Nagatsuta-cho, Midori-ku, Yokohama 226-8503 Japan, Research Institute of Instrumentation Frontier, National Institute of Advanced Industrial Science and Technology (AIST), Central 5, 1-1-1 Higashi, Tsukuba 305-8565 Japan, Department of Chemical System Engineering, The University of Tokyo, 7-3-1, Hongo, Bunkyo-ku, Tokyo 113-8656 Japan, and Kanagawa Academy of Science and Technology, Sakado 3-2-1, Takatsu-ku, Kawasaki 213-0012, Japan

Received May 26, 2008. Revised Manuscript Received October 1, 2008

Sulfonic acid group (SO_3H)-bearing amorphous carbon/mesoporous silica composites were studied for use as solid acid catalysts. Sugar-derived amorphous carbon with SO_3H cannot catalyze hydrophobic acid-catalyzed reactions, such as the dimerization of α-methylstyrene, because of the small surface area. However, SO_3H-bearing sugar-derived amorphous carbon supported on mesoporous silica exhibits remarkable catalytic performance for the dimerization of α-methylstyrene. Under optimal conditions, the selectivity of the composite catalysts for unsaturated dimers exceeds 98%. Structural and reaction analyses revealed that SO_3H-bearing carbon particles with large surface areas are formed in the mesopores and prevent intramolecular Friedel−Crafts alkylation, resulting in high catalytic activity.

Introduction

There has been considerable interest in the development of stable, reusable, and highly active solid acids as environmentally benign replacements for their homogeneous counterparts, such as hydrofluoric and sulfonic acids.[1−7] Production of industrially important chemicals has relied significantly on homogeneous acid catalysts; however, these acid catalysts require special processing in the form of neutralization, involving costly and inefficient catalyst separation from homogeneous reaction mixtures. Solid acid catalysts that are easily separable, reusable, and insoluble acidic solids are one promising candidate for the change from various homogeneous acid catalyst-based processes to more environmentally sensible processes. Such solids can be readily separated from the products and repeatedly reused, thereby minimizing the energy consumption for the production of chemicals. This has stimulated the development of replacement solid catalysts for homogeneous acid catalysts such as sulfated zirconia,[8,9] Cs-exchanged heteropoly acids,[10] acidic polymers,[11] and zeolites.[12] Recently, we reported that a partially carbonized organic compound with a high density of sulfonic acid groups (SO_3H) can function as an efficient solid acid catalyst.[13−16] The material consists of flexible polycyclic carbon nanosheets with SO_3H, COOH, and phenolic hydroxyl (OH) groups in a three-dimensional network that can be readily prepared by partial carbonization of natural organic compounds, such as sugar, cellulose, and starch, followed by sulfonation of the resulting amorphous carbon.[14−16] The carbon material can incorporate large amounts of hydrophilic molecules, including water, into the carbon bulk, because of the high density of hydrophilic functional groups bound to the flexible carbon sheets. This incorporation of hydrophilic molecules provides good access for reactants in solution to the SO_3H groups in the sugar-derived carbon material, which gives rise to high catalytic performance, despite the small surface area (2 $m^2 \cdot g^{-1}$).[16] However, the hydrophilic functional groups prevent incorporation of hydrophobic molecules into the bulk,

* To whom corresponding author should be addressed. Tel: +81-45-924-5381, fax: +81-45-924-5381, e-mail: mhara@msl.titech.ac.jp.
[†] Materials and Structured Laboratory, Tokyo Institute of Technology.
[‡] Chemical Resources Laboratory, Tokyo Institute of Technology.
[§] The University of Tokyo.
[||] National Institute of Advanced Industrial Science and Technology.
[⊥] Kanagawa Academy of Science and Technology.

(1) Anastas, P. T.; Kirchhoff, M. M. *Acc. Chem. Res.* **2002**, *35*, 686.
(2) DeSimone, J. M. *Science* **2002**, *297*, 781.
(3) Harton, B. *Nature* **1999**, *400*, 797.
(4) Anastas, P. T.; Zimmermann, J. B. *Environ. Sci. Technol.* **2003**, *37*, 94A.
(5) Clark, J. H. *Acc. Chem. Res.* **2002**, *35*, 791.
(6) Misono, M. C. R. *Acad. Sci., Ser. IIc* **2000**, *3*, 471.
(7) Harmer, M. A.; Farneth, W. E; Sun, Q. *Adv. Mater.* **1998**, *10*, 1255.
(8) Arata, K.; Matsuhashi, H.; Hino, M.; Nakamura, H. *Catal. Today* **2003**, *81*, 17.
(9) Song, X.; Sayari, A. *Catal. Rev. Sci. Eng.* **1996**, *38*, 329.
(10) Okuhara, T. *Chem. Rev.* **2002**, *102*, 3641.
(11) Harmer, M. A.; Sun, Q. *Appl. Catal., A* **2001**, *221*, 45.
(12) Corma, A. *Adv. Mater.* **1995**, *7*, 137.
(13) Hara, M.; Yoshida, T.; Takagaki, A.; Takata, T.; Kondo, J. N.; Domen, K.; Hayashi, S. *Angew. Chem., Int. Ed.* **2004**, *43*, 2955.
(14) Toda, M.; Takagaki, A.; Okamura, M.; Kondo, J. N.; Hayashi, S.; Domen, K.; Hara, M. *Nature* **2005**, *438*, 178.
(15) Takagaki, A.; Toda, M.; Okamura, M.; Kondo, J. N.; Domen, K.; Hayashi, S.; Hara, M. *Catal. Today* **2006**, *116*, 157.
(16) Okamura, M.; Takagaki, A.; Toda, M.; Kondo, J. N.; Domen, K.; Tatsumi, T.; Hara, M.; Hayashi, S. *Chem. Mater.* **2006**, *18*, 3039.
(17) Harmer, M. A.; Farneth, W. E.; Sun, Q. *J. Am. Chem. Soc.* **1996**, *118*, 7708.
(18) Harmer, M. A.; Sun, Q.; Vega, A. J.; Farneth, W. E.; Heidekum, A.; Földerich, W. F. *Green Chem.* **2000**, *1*, 7.

10.1021/cm801441c CCC: $40.75
Published on Web 12/11/2008

and thereby hydrophobic acid-catalyzed reactions proceed only on surfaces with small surface areas, resulting in poor or no catalytic activity for the reactions. In order to develop active SO_3H-bearing carbon catalysts with large surface areas available for hydrophobic acid-catalyzed reactions, a new strategy was adopted in this study: sulfonation of amorphous carbon deposited in the mesopores of a mesoporous material. It is difficult to prepare highly dispersed SO_3H-bearing carbon particles on large surface area supports such as silica and alumina, because aggregation of impregnated sugar occurs during carbonization through pyrolytic intermediates such as caramel. It has been reported that organic compounds such as sugar can be readily loaded into the mesopores of mesoporous silica such as SBA-15[19,20] and then carbonized without aggregation of the carbon particles in the restricted mesopores.[21] Partial carbonization of sugar loaded onto the walls in silica mesopores, followed by sulfonation, would form small SO_3H-bearing carbon particles with large surface areas that would exhibit high catalytic activity for hydrophobic acid-catalyzed reactions. However, it is unclear whether SO_3H-bearing carbon material with large surface areas available for hydrophobic acid-catalyzed reactions would be formed in such a composite. Sulfonation by sulfuric acid is liable to remove small carbon particles from the silica wall, because of the sulfonation of carbon at the carbon/silica interface. In the case of a large amount of deposited carbon, reactants may have no access to SO_3H on carbon that is plugging up mesopores.

Experimental Section

Preparation of Carbon/SBA-15 Composites. Carbon/SBA-15 composite, a mesoporous silica-supported sulfonated carbon material, was prepared by loading D-glucose into the mesopores of SBA-15. SBA-15 was prepared by hydrolysis of tetramethyl orthosilicate in the presence of a triblock copolymer, P123.[19,20] Two grams of an aqueous solution containing 0.3−1.5 g of D-glucose and 0.14 g of concentrated sulfuric acid was added dropwise to dehydrated SBA-15. The mixture was warmed at 373 K for 24 h and then heated at 433 K for 6 h, allowing the impregnated D-glucose to be partially polymerized and carbonized within the mesopores. Further carbonization was carried out by pyrolysis, with heating of the resulting material at 823 K for 3 h under vacuum. The carbon/silica composite was sulfonated in concentrated H_2SO_4 (96 wt%) with heating at 423 K for 10 h under a N_2 atmosphere. The black powder obtained was completely washed with hot distilled water (>353 K) until sulfate anions were no longer detected. The amount of carbon material loaded in the carbon/SBA-15 composite was estimated by thermogravimetric (TG) analysis. The sample was heated to 1273 K in air, resulting in complete combustion of the carbon material, and the amount of loaded carbon material was obtained from the TG profiles. According to the X-ray photoelectron spectroscopy (XPS) analysis, it was determined that all S atoms in the carbon material were assignable to SO_3H groups.[16] Therefore, the SO_3H acid density was estimated from the S content in each sample composition as determined by elemental analysis.[16]

To obtain carbon material from the carbon/silica composite, the silica was removed using aqueous HF solution. Thirty milliliters of 10% aqueous HF solution was added to 1.0 g of the carbon/silica composite in a Teflon beaker, and the mixture was allowed to stand for 24 h at room temperature. The supernatant solution containing silica was removed, and the black precipitate was washed repeatedly with distilled water until F^- was no longer detected in the wash water.

All procedures for the preparation of the carbon/silica composite and silica removal were performed in a fume food, because of the especially hazardous nature of the concentrated H_2SO_4 and aqueous HF solution reagents.

Hazards. Sulfuric Acid. The corrosive properties of sulfuric acid are accentuated by its highly exothermic reaction with water. Hence, burns from sulfuric acid are potentially more serious than those of comparable strong acids (e.g., hydrochloric acid), as there is additional tissue damage due to dehydration and particularly due to the heat liberated by the reaction with water; i.e. secondary thermal damage.

Hydrogen Fluoride. Hydrofluoric acid is corrosive and a contact poison. It should be handled with extreme care, beyond that accorded to other mineral acids, in part because of its low dissociation constant, which allows HF to penetrate tissue more quickly. Symptoms of exposure to hydrofluoric acid may not be immediately evident. HF interferes with nerve function, and burns may not initially be painful. Accidental exposure can go unnoticed, delaying treatment and increasing the extent and seriousness of the injury. HF is known to etch bone, and since it penetrates the skin, it can essentially destroy bone without destroying the skin.

Characterization. Structural information for the prepared samples was obtained using scanning electron microscopy (SEM), powder X-ray diffraction (XRD, Ultima IV, Rigaku), Raman spectroscopy (NRS-3100, Jasco), N_2 adsorption analysis, and ^{13}C cross-polarization (CP) magic angle spinning (MAS) nuclear magnetic resonance (NMR). SEM images were obtained using an ultra-high-resolution SEM system (S-5200, Hitachi) without metal deposition on the samples. Nitrogen adsorption−desorption isotherms were measured at 77 K using a Micrometrics Coulter SA-3100 system. Prior to the measurement, the samples were pretreated at 423 K for 3 h under vacuum. The Brunauer−Emmett−Teller (BET) surface area was estimated over a relative pressure (P/P_0) range of 0.05 to 0.30. The pore size distribution was obtained from analysis of the adsorption branch of the isotherms using the Barrett−Joyner−Halenda (BJH) method. ^{13}C CP/MAS NMR spectra were measured at room temperature using a Bruker ASX-200 spectrometer at a Larmor frequency of 50.3 MHz. A Bruker MAS probehead was used with a 7 mm zirconia rotor. The spinning rate of the sample was 4.0 kHz. The frequency of the spectra is expressed with respect to pure tetramethylsilane. Experimentally, glycine was used as a second reference material, with a carbonyl signal set at 176.48 ppm.

The acid strength of the carbon/SBA-15 composite was examined using ^{31}P MAS NMR and conventional color-producing reagents.[16] Trimethylphosphine oxide (TMPO)-adsorbed samples were prepared in the liquid phase. Samples dehydrated by evacuation at 423 K for 1 h were soaked in a tetrahydrofuran (THF) solution containing an adequate amount of TMPO at room temperature for 2 days in a glovebox under an Ar atmosphere, followed by evacuation to remove the THF solvent. The TMPO-adsorbed samples were then packed into a rotor in a glovebox under a N_2 atmosphere. ^{31}P MAS NMR spectra for the TMPO-adsorbed samples were measured at room temperature using a Bruker ASX400 spectrometer at a Larmor frequency of 162.0 MHz. The pulse sequence was a single-pulse sequence with high-power proton decoupling. A Bruker MAS probehead was used with a 4 mm

(19) Zhao, D.; Feng, J.; Huo, Q.; Melosh, N.; Fredrickson, H. G.; Chmelka, B. F.; Stucky, G. D. *Science* **1998**, *279*, 548.
(20) Zhao, D.; Huo, Q.; Freng, J.; Chmelka, B. F.; Stucky, G. D. *J. Am. Chem. Soc.* **1998**, *120*, 6024.
(21) Jun, S.; Joo, S. H.; Ryoo, R.; Kruk, M.; Jaroniec, M.; Liu, Z.; Ohsuna, T.; Terasaki, O. *J. Am. Chem. Soc.* **2000**, *122*, 10712.

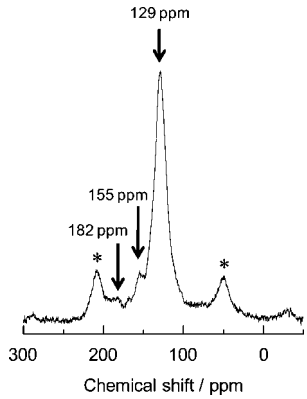

Figure 1. ^{13}C CP/MAS NMR spectra of carbon (20 wt%)/SBA-15 (50.3 MHz). * denotes a spinning sideband.

zirconia rotor. The spinning rate of the sample was 8 kHz. The ^{31}P chemical shift was referenced to 85% H_3PO_4 at 0.0 ppm. Experimentally, $(NH_4)_2HPO_4$ was used as a second reference material, the signal of which was set at 1.33 ppm. In the case of acidity measurement using color-producing reagents,[16] as the coloration of the reagents cannot be observed by inspection on these black carbon materials, the acidity was examined by ultraviolet−visible diffuse reflectance spectroscopy (UV−vis DRS; V560, Jasco). A mixture of the carbon material (0.2 g) and $BaSO_4$ (reference material, 1.0 g) powder was evacuated at 423 K for 1 h to remove adsorbed water. The mixture was packed into a sealable quartz cell in an Ar-filled glovebox, and benzene (with or without color-producing reagent) was then added to the cell. DRS spectra of the mixture in each benzene solution were measured without exposure to air. The DRS of the color-producing reagent in the presence of the carbon material was obtained by subtracting the spectrum for the mixture in pure benzene from that of a mixture of the color-producing reagent in benzene solution.[16] The DRS for each color-producing reagent was also observed using $BaSO_4$ in benzene, with and without the color-producing reagent, in a similar manner.[16]

Acid-Catalyzed Reaction. Acid catalysis of the carbon/SBA-15 composite was demonstrated by the dimerization of α-methylstyrene (AMS) (323 K). For comparison, sulfuric acid, ion-exchanged resin (Nafion-NR50, Nafion-SAC13, and Amberlyst-15), and a conventional D-glucose-derived carbon-based solid acid[17] were also tested for the same acid-catalyzed reaction. Prior to reaction, all catalysts except sulfuric acid were dehydrated by heating at 373−453 K for 1 h. Dimerization of AMS was performed in a Pyrex flask equipped with a water-cooler condenser. AMS (25 mmol) was reacted over the catalyst (0.2 g) at 373 K for 4 h. Samples were withdrawn at intervals from the reaction mixtures and analyzed by gas chromatography using a capillary column.

Results and Discussion

Structure of the Carbon/SBA-15 Composite. Figure 1 shows the ^{13}C CP/MAS NMR spectrum for the carbon/SBA-15 composite (carbon (20 wt%)/SBA-15) prepared by sulfonation of 20 wt% amorphous carbon supported on SBA-15. Three resonance peaks appear at 129, 155, and 182 ppm, which are assignable to polycyclic aromatic carbons, phenolic OH, and COOH, respectively.[16] The peak due to aromatic carbon with SO_3H groups (Ar-SO_3H, ca. 140 ppm) is not observed in the spectrum. The resonance derived from Ar-SO_3H is not distinguished in the spectra of SO_3H-bearing amorphous carbon samples, because broad peaks due to aromatic carbon atoms (129 ppm) and OH groups (155 ppm) obscure the peak (see below).[16]

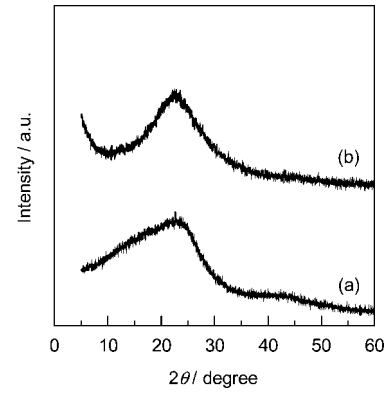

Figure 2. XRD patterns for (a) the bulky glucose-derived carbon material and (b) carbon (20 wt%)/SBA-15.

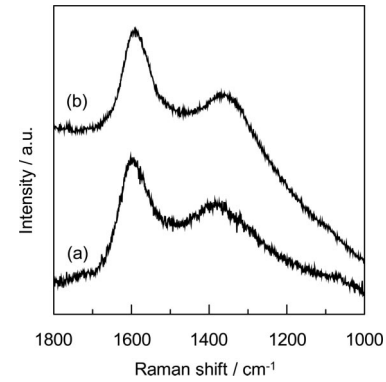

Figure 3. Raman spectra for (a) the bulky glucose-derived carbon material and (b) carbon (20 wt%)/SBA-15.

Figures 2 and 3 show XRD patterns and Raman spectra for the bulky glucose-derived carbon material and carbon/silica composite, respectively. The broad but weak diffraction peaks in the XRD patterns at 2θ angles of 10−30° (C(002)) are attributable to amorphous carbon composed of aromatic carbon sheets oriented in a considerably random fashion.[22] In the Raman spectra, the intensity ratios of the D band (1350 cm^{-1}, A_{1g} D breathing mode) to the G band (1580 cm^{-1}, E_{2g} G mode) for the bulky glucose-derived carbon material and carbon/silica composite are 0.8, indicating that the average graphene size in both carbon materials is ca. 1 nm.[23] There is no significant difference between the XRD and Raman data for the bulky glucose-derived carbon material and carbon/silica composite.

Figure 4 shows SEM images of SBA-15 and the carbon/SBA-15 composite, before and after the removal of silica using a 10 wt% HF solution. SEM images of the parent SBA-15 clearly show the formation of entirely rod-like macrostructures (Figure 4A) and a two-dimensional hexagonal mesoporous structure with uniform pores (Figure 4B). There was no significant difference between the surface morphology of SBA-15 and the carbon (20 wt%)/SBA-15 composite (Figure 4C), despite large amounts of deposited carbon. It was confirmed by XPS that the introduced carbon is not deposited on the SBA-15 surface. The SEM image of carbon (33 wt%)/SBA-15 (Figure 4D) also shows the original porous structure, indicating no blockage of the mesopores by

(22) Tsubouchi, N.; Xu, K.; Ohtsuka, Y. *Energy Fuels* **2003**, *17*, 1119.
(23) Ferrari, A. C.; Robertson, J. *Phys. Rev. B* **2000**, *61*, 14095.

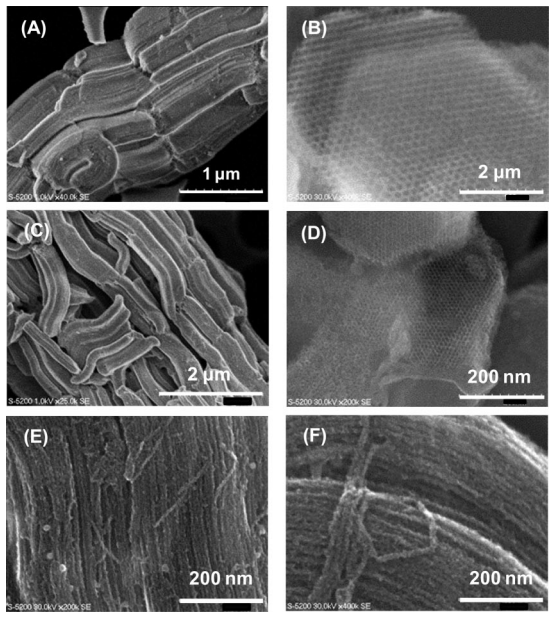

Figure 4. SEM images of (A, B) parent SBA-15, (C) carbon (20 wt%)/SBA-15, (D) carbon (33 wt%)/SBA-15, and (E, F) carbon obtained by silica removal from carbon (20 wt%)/SBA-15.

sulfonated carbon nanoparticles. The ^{13}C MAS NMR spectrum for the carbon material, obtained by the removal of silica from carbon (20 wt%)/SBA-15, was consistent with that of carbon (20 wt%)/SBA-15 (Figure 1), and the photoelectron peak of S2p due to SO_3H (168 eV) was observed in the XPS spectrum. These results indicate that most of the impregnated D-glucose is incorporated into SBA-15 by capillary action and is converted into SO_3H-bearing carbon fixed in the mesopores of the SBA-15 mold. Carbon loading beyond 50 wt% under the same preparative conditions resulted in the deposition of carbon on the external surface of SBA-15.

N_2 adsorption−desorption isotherms of SBA-15 and the carbon/SBA-15 composites after sulfonation are shown in Figure 5A. The isotherm of SBA-15 (a in Figure 5A) is a typical type-IV pattern with a clear H1-type hysteresis loop at high relative pressures. The H1 hysteresis loop, representing a parallel and nearly vertical branch of the adsorption−desorption isotherm, has been shown to be characteristic of materials with cylindrical pore geometry and highly uniform pore size. The original H1 hysteresis loop is maintained for 13 and 20 wt% carbon-loaded SBA-15, suggesting that the sulfonated carbon is deposited as a uniform coating on the mesopore without pore blockage. The hysteresis loop clearly disappears in the isotherm of the carbon (33 wt%)/SBA-15 sample, indicating that the introduction of excess carbon into SBA-15 plugs the mesopore channels. The structural properties and the SO_3H density of the samples are summarized in Table 1. The sulfonic acid groups in the composite increase with increasing amount of deposited carbon-bearing SO_3H. In the case of a large amount of deposited carbon (carbon (33−43 wt%)/SBA-15), the carbon material plugs the mesopores; however, these samples do maintain a large surface area. It has been reported that sugars loaded into mesopores are carbonized with contraction, resulting in the formation of vacancies between the carbon rods and the walls of the mesopores.[24] The large surface areas of the SBA-15 composites plugged with carbon can be attributed to these vacancies. The N_2 adsorption−desorption isotherm of the SO_3H-bearing carbon obtained by silica removal from carbon (20 wt%)/SBA-15 exhibits a type-I pattern, as shown in Figure 5B, which is typical for a microporous solid; the H1 hysteresis loop observed for the carbon (20 wt%)/SBA-15 (c in Figure 5A) is clearly not present. The carbon material obtained by silica removal from the carbon/silica composite shows a hysteresis loop at P/P_0 of ca. 0.5, as observed for CMK-5 interconnected thin carbon nanopipes.[25] However, the isotherm for the carbon material itself is similar to that of a type-I pattern, suggesting that the carbon material obtained by silica removal is not identical to CMK-5. In the case of SO_3H-bearing carbon/SBA-15 prepared by heating a small amount of D-glucose incorporated into the mesopores at lower temperature, rigid carbon pillars may not form; the carbon material in the mesopores aggregate without the formation of rigid carbon pillars, and the mesopores disappear after the removal of silica. Despite the disappearance of the mesoporous structure, the SO_3H-bearing carbon still has a large surface area (992 $m^2 \cdot g^{-1}$) and pore volume (0.50 $mL \cdot g^{-1}$), indicating that partial carbonization of sugar loaded onto the silica walls in the mesopores, followed by sulfonation, forms large surface area SO_3H-bearing carbon that is fixed on the silica walls.

The acid strength of the solid acid catalysts was evaluated using ^{31}P MAS NMR experiments on samples treated with TMPO as a basic probe molecule.[26] The advantage of using phosphorus molecules over other basic probes, such as pyridine and acetonitrile, is associated with the higher sensitivity and wider chemical shift range of ^{31}P resonance in the NMR spectrum.[27] It is well-established that the peak position of TMPO adsorbed on the Brønsted acid site is downshifted and the degree of peak shift is directly dependent on the acid strength of the catalyst.[28−30] ^{31}P MAS NMR spectra of carbon (20 wt%)/SBA-15 (a), and carbon obtained by silica removal from carbon (20 wt%)/SBA-15 after TMPO adsorption, are displayed in Figure 6. Three distinct signals at 86, 79, and 51 ppm are clearly observed in the spectrum of carbon (20 wt%)/SBA-15 (Figure 6a). The signal at 40 ppm, assignable to the self-aggregated TMPO on the solid surface, is not present, indicating that TMPO can diffuse in the nanospaces of the carbon/silica composites, and all of the introduced TMPO molecules are adsorbed on acid sites.[16] The strong signal at 51 ppm is derived from TMPO adsorbed on the silanol (Si-OH),[28,30] which is overlapped with the signals for TMPO adsorbed on COOH and phenolic OH

(24) Ogura, M.; Zhang, Y.; Elangovan, S. P.; Okubo, T. *Microporous Mesoporous Mater.* **2007**, *101*, 224.
(25) Kruk, M.; Jaroniec, M.; Kim, T.-W.; Ryoo, R. *Chem. Mater.* **2003**, *15*, 2815.
(26) Baltusis, L.; Frye, J. S.; Maciel, G. E. *J. Am. Chem. Soc.* **1987**, *109*, 40.
(27) Maciel, G. E.; Ellis, P. D. In *NMR Technique in Catalysis*; Bell, A. T., Pines, A., Eds.; Marcel Dekker: New York, 1994; pp 231−309.
(28) Rakiewicz, E. F.; Peters, A. W.; Wormsbecher, R. F.; Sutovich, K. J.; Mueller, K. T. *J. Phys. Chem. B* **1998**, *102*, 2890.
(29) Karra, M. D.; Sutovich, K. J.; Mueller, K. T. *J. Am. Chem. Soc.* **2002**, *124*, 902.
(30) Zhao, Q.; Chen, W.-H.; Huang, S.-J.; Wu, Y.-C.; Lee, H.-K.; Liu, S.-B. *J. Phys. Chem. B* **2002**, *106*, 4462.

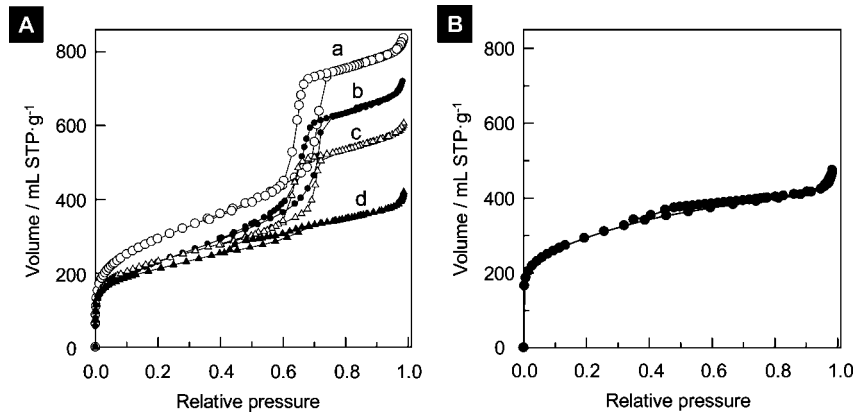

Figure 5. N_2 adsorption−desorption isotherms of (A) the carbon/SBA-15 composites and (B) carbon obtained by silica removal from carbon (20 wt%)/SBA-15 using 10% aqueous HF solution. (a) Parent SBA-15, (b) carbon (13 wt%)/SBA-15, (c) carbon (20 wt%)/SBA-15, and (d) carbon (33 wt%)/SBA-15.

Table 1. Structural Characteristics of the Carbon/SBA-15 Composites

	carbon content[a]/wt%	S_{BET}/m^2·g^{-1}	pore volume/mL·g^{-1}	pore size/nm	SO_3H density[b]/mmol·g^{-1}
SBA-15	0	1020	1.4	7.1	0
carbon (13 wt%)/SBA-15	13	1020	1.2	6.8	0.11
carbon (20wt%)/SBA-15	20	760	1.0	7.0	0.13
carbon (33 wt%)/SBA-15	33	700	0.5	−	0.30
carbon (38 wt%)/SBA-15	38	660	0.4	−	0.36
carbon (43 wt%)/SBA-15	43	690	0.4	−	0.38
carbon material obtained by silica removal from carbon (20 wt%)/SBA-15[c]	−	992	0.5	−	0.80

[a] Carbon content in catalysts was estimated by thermogravimetric (TG) analysis. [b] Acid densities were estimated from the S content in sample compositions determined by elemental analysis. [c] The sample was obtained by silica removal from carbon (20 wt%)/SBA-15.

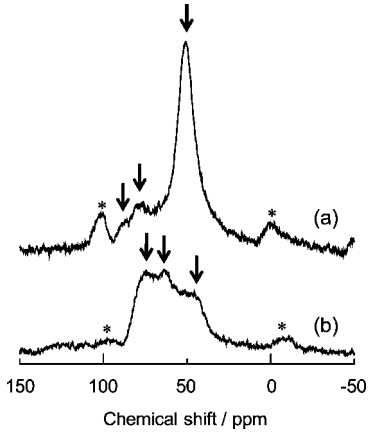

Figure 6. ^{31}P MAS NMR spectra for (a) carbon (20 wt%)/SBA-15 and (b) carbon obtained by silica removal from carbon (20 wt%)/SBA-15 after TMPO adsorption. The SO_3H/TMPO ratio of samples is 2. * denotes a spinning sideband.

groups (40−75 ppm).[16] Because TMPO signals with a strong Brønsted acid site appear at around 78−86 ppm (H-β: 78 ppm,[31] Amberlyst-15: 81 ppm, and H-ZSM-5: 86 ppm[28]), two signals at higher chemical shift (79 and 86 ppm) can be reasonably assigned to SO_3H groups. In our previous report, the chemical shift for TMPO-adsorbed bulky SO_3H-bearing amorphous carbon prepared from D-glucose appeared at 81 ppm,[16] indicating that the carbon/SBA-15 composite has stronger Brønsted acid sites than bulky SO_3H-bearing carbon material. In the case of carbon obtained by silica removal from carbon (20 wt%)/SBA-15, the broad signals centered at around 75, 64, and 45 ppm are observed and are attributable to TMPO-adsorbed SO_3H, TMPO-adsorbed COOH or OH, and physisorbed TMPO, respectively. Apparently, the strongest acid sites observed for the carbon/SBA-15 composite are not present in the carbon. Although such enhancement in acid strength on a silica support has been found in Nafion and silica-supported Nafion,[17] the details remain to be clarified. The acidities of the carbon/silica composites were also examined using color-producing reagents.[16] A broad absorption band appears at 450−600 nm in the spectrum for each carbon/silica composite dyed with anthraquinone, attributable to the yellow coloration of anthraquinone in strong acid ($pK_a \leq -8.2$), whereas the yellow coloration of *p*-nitrotoluene ($pK_a \leq -11.4$) is not observed. This indicates that SO_3H in the carbon/silica composite has a pK_a of −11 to −8, corresponding to acidity comparable to that of concentrated H_2SO_4. This is consistent with the ^{31}P MAS NMR results.

Catalytic Performance of Carbon/SBA-15 Composite. The catalytic performance of the carbon/silica solid acids has been demonstrated through the dimerization of AMS.[31−35] Acid-catalyzed dimerization of AMS produces a mixture of unsaturated dimers (2,4-diphenyl-4-methyl-1-pentene (**III**) and 2,4-diphenyl-4-methyl-2-pentene (**IV**)) and a saturated dimer (1,1,3-trimethyl-3-phenylindan (**V**)), as shown in

(31) Kao, H.-M.; Yu, C.-Y.; Yeh, M.-C. *Microporous Mesoporous Mater.* **2002**, *53*, 1.
(32) Chaudhuri, B.; Sharma, M. M. *Ind. Eng. Chem. Res.* **1989**, *28*, 1757.
(33) Fujiwara, M.; Kurokawa, K.; Yazawa, T.; Xu, Q.; Tanaka, M.; Souma, Y. *Chem. Commun.* **2000**, *16*, 1523.
(34) Sun, Q.; Farneth, W. E. *J. Catal.* **1996**, *164*, 62.
(35) Fujiwara, M.; Terashima, S.; Endo, Y.; Shiokawa, K.; Ohue, H. *Chem. Commun.* **2006**, *44*, 4635.

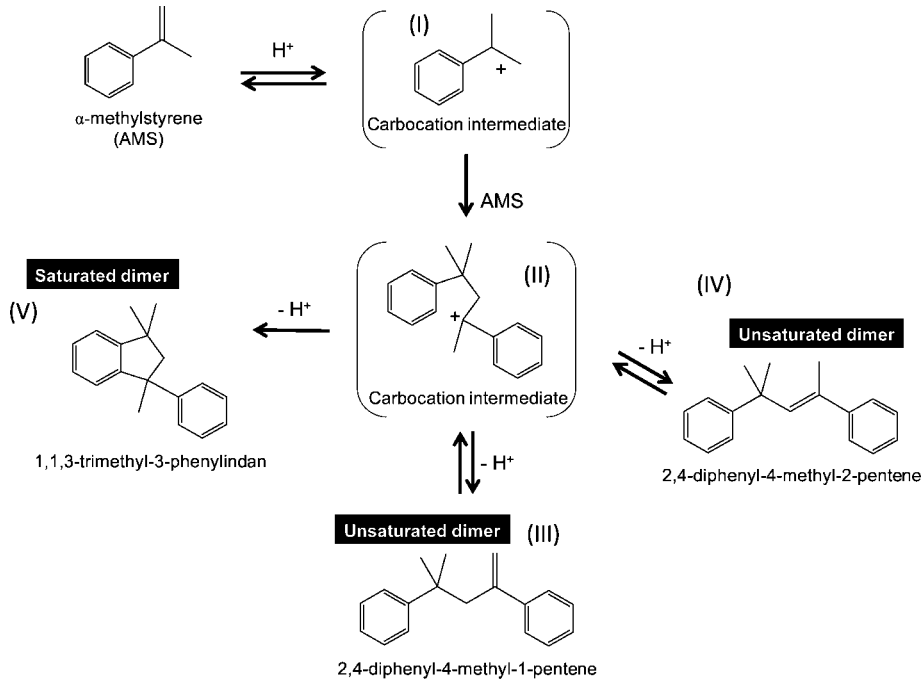

Figure 7. Reaction mechanism for AMS dimerization.

Table 2. Catalytic Activity of the Catalysts Tested for Dimerization of α-Methylstyrene at 323 K

catalyst	S_{BET}/m^2·g^{-1}	SO_3H density[b]/mmol·g^{-1}	acidity/H_0	conversion[d]/%	selectivity[e]/%	rate/mmol·g^{-1}·min^{-1}	TOF[f]/min^{-1}
glucose-derived carbon	2	0.70	−8 to −11[c]	trace	trace	trace	trace
carbon (20 wt%) /SBA-15	723	0.13	−8 to −11[c]	86	99	1.3	9.8
carbon (38 wt%) /SBA-15	610	0.34	−8 to −11[c]	85	98	1.8	5.4
carbon material obtained by silica removal from carbon (20wt%)/SBA-15[a]	992	0.80	−8 to −11[c]	85	95	0.7	1.5
Amberlyst-15	50	4.90	−2.2	74	50	1.8	0.4
Nafion NR50	<1	0.90	−11 to −13	4.7	93	trace	trace
Nafion SAC13	344	0.13	<−12.2	86	40	2.1	16.4

[a] The sample was obtained by silica removal from carbon (20 wt%)/SBA-15. [b] Acid densities of SO_3H were estimated from the S content in sample compositions determined by elemental analysis. [c] The acidities were measured using color producing reagents.[6] [d] Reaction time: 1 h. [e] Selectivity for unsaturated dimers. [f] TOF was estimated from the initial rate per acid sites.

Figure 7. The unsaturated dimer **III** synthesized by this reaction is an industrially important chemical as a chain-transfer agent or molecular weight regulator in the syntheses of acrylonitrile−butadiene−styrene (ABS) resin and styrene−butadiene-rubber (SBR). In the catalytic reaction shown in Figure 7, protonated AMS **I** is reacted with an AMS monomer to form a dimeric carbocation intermediate (**II**). It has been reported that the dimeric carbocation intermediate **II** plays a critical role in this reaction; the carbocationic dimer **II** is transformed into two dimeric pentene derivates **III** and **IV** by equilibrium reactions, and irreversibly into the cyclic indan derivate **V** by intramolecular Friedel−Crafts alkylation. It is necessary to inhibit the formation of the indan derivative **V** in order to selectively synthesize the unsaturated dimer **III**.

The catalytic activity of the catalysts tested for the reaction is summarized in Table 2. The results for a bulky glucose-derived carbon solid acid,[16] Nafion resin (NR50),[11] Nafion-silica composite (SAC-13),[17,18] Amberlyst-15,[11] and sulfuric acid are included for comparison. 0.2 g of each catalyst was used for the reaction. Nafion NR50, SAC-13 and Amberlyst-15 are polymer-based strong solid acids with high densities of SO_3H, and very high activity for a variety of reactions.[11,17,18] In the presence of sulfuric acid, most of the AMS is converted into the worthless cyclic indan derivate **V** within a short reaction time, and the combined selectivity for the useful dimers **III** and **IV** is only 13%. While Nafion resin (NR50) cannot function as an efficient catalyst for the reaction, because of its small surface area, the Nafion-silica composite (SAC-13) and Amberlyst-15 with relatively large surface areas have better AMS conversion. The selectivity for the dimeric pentene derivatives of these two conventional solid acids reaches 50% and 40%, respectively, indicating that these resin catalysts form the saturated indan in parallel with formation of the unsaturated dimers, as is the case for sulfuric acid. In contrast to the conventional acid catalysts, carbon/SBA-15 exhibits remarkable catalytic performance; the AMS conversion and dimeric pentene selectivity exceed 85% and 95%, respectively. There is no significant difference in conversion and selectivity between carbon (20 wt%)/SBA-15 and (38 wt%)/SBA-15, and the turnover frequency (TOF) of the former is larger than that of the latter. This is indicative of a decrease in effective SO_3H groups for the reaction (i.e., surface SO_3H on the carbon material) with enlarging carbon particle size. It was confirmed that the SBA-15 support has no catalytic activity for the reaction, indicating that silanol groups do not take part in the reaction. After completion of the reaction, the carbon/silica composite could be readily

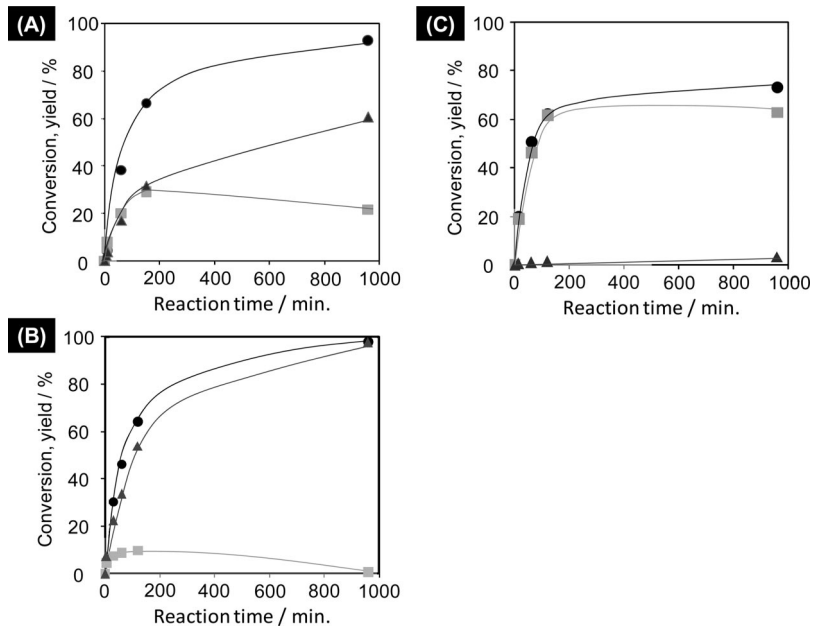

Figure 8. Time courses of 2,4-diphenyl-4-methyl-1-pentene conversion (●) and yields of 2,4-diphenyl-4-methyl-2-pentene (■) and 1,1,3-trimethyl-3-phenylindan (▲) over Amberlyst-15 (A), Nafion SAC-13 (B), and carbon (20 wt%)/SBA-15 (C).

separated from the reaction solution. No decrease in activity was observed even after three reuses of the same sample (carbon (20 wt%)/SBA-15), and elemental analyses of the carbon material and the reaction solution revealed that leaching of SO_3H groups from the composite did not occur during the reactions. Neither the bulky glucose-derived carbon material nor physical mixtures of the bulky carbon material (0.02−0.10 g) and SBA-15 or amorphous silica CABOSIL (0.10 g) catalyzed the reaction. This is because the carbon material cannot incorporate hydrophobic molecules such as AMS into the bulk structure, which possesses most of the SO_3H groups, and the surface area ($2\ m^2 \cdot g^{-1}$) with the SO_3H groups is too small to catalyze the reaction.

Catalytic capability for intramolecular Friedel−Crafts alkylation, which is strongly related to the high selectivity for unsaturated pentenes, was tested using 2,4-diphenyl-4-methyl-1-pentene (**III**) as a reactant over sulfonic acid-bearing solid acid catalysts (Amberlyst-15, Nafion-silica composite, and carbon (20 wt%)/SBA-15). Figure 8 shows time courses of 2,4-diphenyl-4-methyl-1-pentene (**III**) conversion and the yields of 2,4-diphenyl-4-methyl-2-pentene (**IV**) and 1,1,3-trimethyl-3-phenylindan (**V**) over these catalysts. Most of the unsaturated 1-pentene **III** was converted over all the catalysts with a short reaction time at 333 K. Both unsaturated 2-pentene **IV** and saturated cyclic indan **V** were comparably evolved over Amberlyst-15 in the initial stage of the reaction; however, the amount of unsaturated 2-pentene **IV** evolved gradually decreased after 3 h, indicating that the intramolecular Friedel−Crafts alkylation proceeded continuously. In the case of Nafion SAC-13, the saturated cyclic indan **V** was predominantly formed during reaction. Unsaturated 2-pentene **IV** formed at the early stage of the reaction decreases with reaction time and was not observed after 16 h; the intramolecular Friedel−Crafts alkylation is the predominant reaction over Nafion SAC-13. In contrast to these conventional solid acid catalysts, most of the reacted unsaturated 1-pentene **III** was converted to unsaturated 2-pentene **IV** over the carbon/SBA-15 composite by acid-catalyzed transformation. As a result, the selective production of unsaturated 2-pentene **IV** in the AMS dimerization by the carbon/SBA-15 composite can be attributed to the blocking of intramolecular Friedel−Crafts alkylation. The difference in the catalytic properties of sulfonic acid-bearing catalysts for the production of dimeric pentenes cannot adequately be explained as being due solely to factors such as surface area or acid strength, because other acid catalysts with similar or higher surface areas and acidity do not prevent indan formation, as shown in Table 2. The SO_3H-bearing carbon, obtained by the removal of silica from carbon (20 wt%)/SBA-15, also shows high selectivity for dimeric pentene production, although the TOF for this carbon material is moderate, due to degradation of the carbon by HF during removal of the silica. This means that the selective production of dimeric pentene over the carbon/SBA-15 composite is attributed to the SO_3H-bearing carbon itself. To investigate the catalysis of the carbon/SBA-15 composite, sulfonated active carbon was prepared and examined. An activated carbon ($1050\ m^2\ g^{-1}$) heated at 873 K for 3 h under vacuum (<1 Pa) was sulfonated in concentrated H_2SO_4 with heating at 423 K for 10 h under a N_2 atmosphere, resulting in sulfonated active carbon. The surface area and SO_3H density of the carbon material were $980\ m^2\ g^{-1}$ and 0.53 mmol g^{-1}, respectively. OH and COOH groups were not observed on the sulfonated-active carbon by ^{13}C CP/MAS NMR. Although the sulfonated active carbon has a larger surface area and higher SO_3H density than the carbon/SBA-15 composite, the carbon material exhibits only moderate catalytic performance for the dimerization of α-methylstyrene, with conversion and selectivity for unsaturated dimers at 53 and 42%, respectively, under the reaction conditions indicated in Table 2. As a result, the selective production of dimeric pentene over the carbon/SBA-15 composite cannot be explained by only SO_3H groups bonded to carbon sheets. The carbon material possesses COOH and phenolic OH

groups in addition to the strong Brønsted acid sites (SO_3H). This is distinct from conventional solid acids with single functional groups, including the prepared sulfonated activated carbon. Recently, we found that bulky amorphous carbon bearing SO_3H, COOH, and phenolic OH functions as an effective solid catalyst for the hydrolysis of cellulose into glucose.[36] In the reaction, SO_3H groups hydrolyze cellulose bonded to the carbon surface through phenolic OH groups. The synergetic catalysis has remarkable catalytic performance for the reaction. The results for sulfonated active carbon suggest that phenolic OH or COOH groups bonded to carbon sheets in the carbon/SBA-15 composite also participate in the reaction, and the synergetic effect of these functional groups results in the efficient and selective production of dimeric pentene. The relationship between the assembly of functional groups on the carbon material and the mechanism of catalysis is currently under investigation.

Conclusion

Partial carbonization and sulfonation of D-glucose-impregnated SBA-15 resulted in the formation of a carbon/SBA-15 composite, where SO_3H-bearing carbon with large surface area is incorporated into the mesopores of SBA-15. Bulky SO_3H-bearing carbon material, prepared simply by the partial carbonization and sulfonation of D-glucose, does not catalyze the dimerization of α-methylstyrene at all because of the small surface area, while the carbon/SBA-15 composite exhibits remarkable catalytic performance (conversion and selectivity) for the production of dimeric pentene derivates from α-methylstyrene. The selective production of unsaturated dimers over the carbon/SBA-15 composite can be attributed to blocking of the intramolecular Friedel−Crafts alkylation on SO_3H-bearing carbon with large surface area.

Acknowledgment. This work was supported by the New Energy and Industrial Technology Development Organization (NEDO, 04A32502), the Research and Development in a New Interdisciplinary Field Based on Nanotechnology and Materials Science programs of the Ministry of Education, Culture, Sports, Science and Technology (MEXT) of Japan, and a Grant-in-Aid for Scientific Research (18206081) from the Japan Society for the Promotion of Science (JSPS).

CM801441C

(36) Suganuma, S.; Nakajima, K.; Kitano, M.; Yamaguchi, D.; Kato, H.; Hayashi, S.; Hara, M. *J. Am. Chem. Soc.* **2008**, *130*, 12787.